processes

MDPI

Article

Phytochemicals from *Piper betle* (L.) as Putative Modulators of a Novel Network-Derived Drug Target for Coronary Artery Disease: An In Silico Study

Sudhan [1], Janakiraman [1], Sheikh F. Ahmad [2], Abubakar Wani [3] and Shiek S. S. J. Ahmed [1,*]

[1] Drug Discovery and Multiomics Laboratory, Faculty of Allied Health Sciences, Chettinad Academy of Research and Education, Chettinad Hospital and Research Institute, Kelambakkam 603103, Tamil Nadu, India
[2] Department of Pharmacology and Toxicology, College of Pharmacy, King Saud University, Riyadh 11451, Saudi Arabia
[3] Department of Immunology, St. Jude Children's Research Hospital Memphis, Memphis, TN 38105, USA
* Correspondence: shiekssjahmed@gmail.com

Abstract: Coronary artery disease (CAD) is a leading cause of death worldwide. Despite effective anti-CAD drugs, the rising mortality suggests that more pharmacological targets need to be discovered to improve treatment effectiveness. This study explores and evaluates traditional medicinal plant (*Piper betle* (L.)) compounds against a new target identified through protein network analysis. Our network analysis suggests that the GRB2 protein could be a potential target that links most of the pathological pathway-related proteins in CAD. As a result, we evaluated potential compounds from *Piper betle* (L.) through ADMET (absorption, distribution, metabolism, excretion, and toxicity) profiling, docking, and molecular dynamics (MDs) simulation against the GRB2. The ADMET screening detected 49 druggable phytochemicals in *Piper betle* (L.). Further, screening through molecular docking showed that piperbetol has a higher predicted affinity towards the dimeric form of GRB2 (−8.10 kcal/mol) than other analyzed phytochemicals. Additionally, MD simulation demonstrated that piperbetol formed a stable complex with GRB2 during the simulation. In conclusion, piperbetol from *Piper betle* showed favorable binding with the identified CAD target. Further investigations are needed for pharmaceutical translation.

Keywords: coronary artery disease; *Piper betle* (L.); protein–protein interaction; docking; molecular dynamics simulation

Citation: Sudhan; Janakiraman; Ahmad, S.F.; Wani, A.; Ahmed, S.S.S.J. Phytochemicals from *Piper betle* (L.) as Putative Modulators of a Novel Network-Derived Drug Target for Coronary Artery Disease: An In Silico Study. *Processes* **2023**, *11*, 3064. https://doi.org/10.3390/pr11113064

Academic Editors: Outi Salo-Ahen, Parthiban Marimuthu and Bing-Huei Chen

Received: 26 September 2023
Revised: 11 October 2023
Accepted: 23 October 2023
Published: 25 October 2023

1. Introduction

Coronary artery disease (CAD) is an inflammatory condition characterized by the manifestation of stable and unstable angina that constricts the heart blood vessels [1]. According to the World Health Organization (WHO), CAD accounts for 7 million deaths and 129 million morbidities worldwide [2]. The prevalence of CAD is contributed to by risk factors, including age, ethnicity, family history, lifestyle, smoking, and obesity [3]. Among the reported risk factors, lifestyle modifications and genetic factors play critical roles in the pathogenesis of CAD [4]. At present, several drugs have been recommended to treat and prevent CAD, which include statins (which lower cholesterol levels), ACE inhibitors and beta blockers (which lower the blood pressure), fibrates (which lower triglycerides), calcium channel blockers (which increase oxygen to the heart), and platelet inhibitors (which suppress blood clotting mechanisms). These drugs are clinically approved and recommended for the long-term treatment of CAD [5]. Despite the fact that these medications work well, a high mortality rate raises the possibility that there are more possible pharmacological targets that need to be discovered in order to improve treatment effectiveness. As a result, the current study is focused on identifying the most optimal pharmacological target via

protein network analysis, and to discover potent modulators from a traditional medicinal plant against the putative target in order to delay or stop the pathological process of CAD.

Recently, medicinal plants have grabbed the attention of many researchers for developing novel, effective drugs against complex diseases [6]. Particularly, plant-derived compounds are the best choices due to their low cost, abundance, and low toxicity [7]. Additionally, phytochemicals from traditional plants are demonstrated to be a better alternative to synthesized drugs in a variety of diseases. Nayaka et al., 2021, reported that the ancient Indian medicinal plant *Piper betle* (L.) was traditionally used for vaginal douching, gargle mouthwash, dental problems, headaches, arthritis, joint pain, and cough medicine [8]. Murugesan et al., 2020, reported the anti-inflammatory and antioxidant activities of *Piper betle* (L.) against rheumatoid arthritis in rat models [9]. Similarly, Ng et al., 2014, demonstrated the cytotoxic effect of *Piper betle* (L.) extract on inhibiting colon cancer [10]. Interestingly, Arya et al., 2010, demonstrated the cardioprotective effect of *Piper betle* (L.) extract on lipid peroxidation, restoring endogenous antioxidants, hemodynamics, and left ventricular functions in myocardial infarction [11]. Notably, most of these investigations are carried out on *Piper betle* (L.) extract without disclosing the potential compounds or phytochemicals against diseases. Hence, the screening of *Piper betle* (L.) phytochemicals against the CAD target will help identify potential lead molecules for CAD treatment, which may avoid adverse effects and improve the quality of life.

This study uses a computational approach to identify the potential CAD protein target by integrating the reported CAD genes from a variety of databases to construct the protein network. Such a protein network was inferred to establish the core interconnected proteins that might be involved in the development of CAD. Our analysis establishes the growth-factor-receptor-bound protein 2 (GRB2) as a putative target based on protein connectivity, biological processes, and signaling pathways. The compounds derived from *Piper betle* (L.) were computationally examined with regard to their absorption, distribution, metabolism, excretion, and toxicity (ADMET). Molecular docking and consequent molecular dynamics (MD) simulation suggested that piperbetol from *Piper betle* (L.) has a favorable binding interaction with GRB2. Figure 1 illustrates the complete approach that was designed to find the target and the phytochemicals.

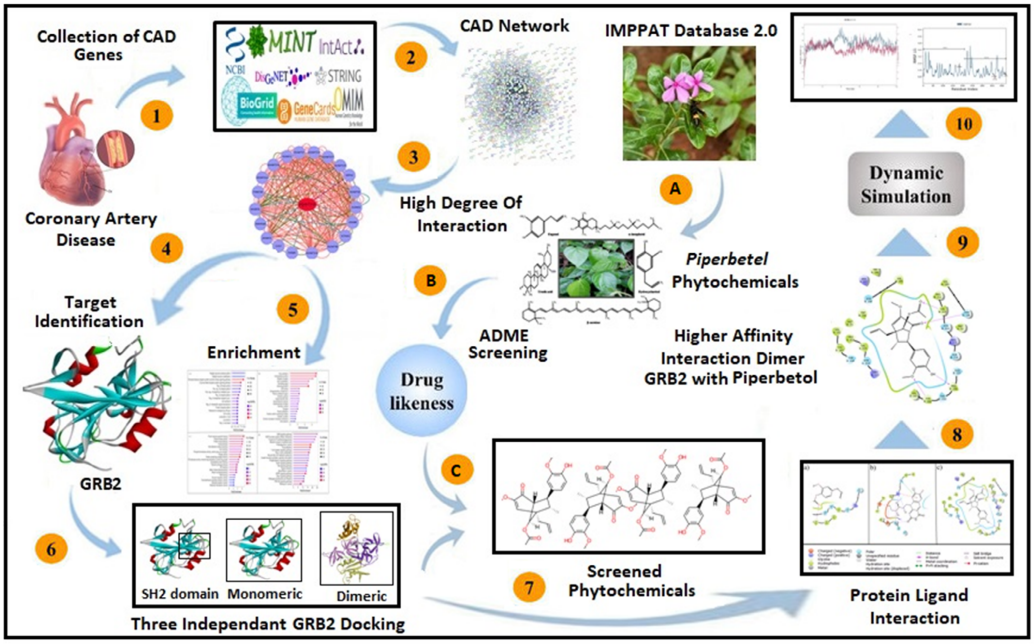

Figure 1. Complete workflow of the current investigation: 1. Network construction and CAD target identification (Steps 1 to 5); 2. phytochemical collection and ADMET screening (Steps A to C); 3. docking and MD simulation (Steps 6 to 10).

2. Materials and Methods

2.1. Collection and Construction of the CAD Network

CAD-associated genes were retrieved from multiple resources, including NCBI (https://www.ncbi.nlm.nih.gov/gene, accessed on 30 June 2023), DisGenet (https://www.disgenet.org/search, accessed on 1 July 2023), OMIM (https://www.omim.org/, accessed on 3 July 2023), GeneCards (www.genecards.org, accessed on 5 July 2023), intAct (https://www.ebi.ac.uk/intact, accessed on 7 July 2023), MINT (https://mint.bio.uniroma2.it, accessed on 9 July 2023), BioGRID (https://thebiogrid.org, accessed on 12 July 2023), and String databases (https://string-db.org, accessed on 15 July 2023). A variety of key terms related to "coronary artery disease" were used to search each database to retrieve gene symbols. The extracted gene symbols of each database were integrated and converted into official symbols to remove duplicates. Cytoscape 3.9.1 with the plug-in was used to construct the protein interaction network with the extended proteins from the initial set retrieved from the databases.

2.2. Network Assessment and Enrichment Analysis

The constructed network was dissected to investigate the hubs with a high degree of connectivity. From the list of hubs, the top hub with high connectivity was selected and subjected to the Shinygo tool (http://bioinformatics.sdstate.edu/go76/, accessed on 29 July 2023) for functional enrichment analysis. Shinygo is an open web server providing a complete collection of functional annotation tools to understand the biological significance behind inputted genes/proteins. Herein, the functional enrichment of the proteins in the selected hub was assessed based on cellular components (CC), biological processes (BP), molecular function (MF), and molecular pathways for their relevance in CAD pathogenesis.

2.3. Ligand Collection and ADMET Profiling

IMPPAT: Indian Medicinal Plants, Phytochemistry, and Therapeutics (https://cb.imsc.res.in/imppat/, (accessed on 2 August 2023) database [12] was used to collect the list of *Piper betle* (L.) phytochemicals, and their structures were retrieved from the IMPPAT database (https://cb.imsc.res.in/imppat/, accessed on 3 August 2023) in Structure Data File (SDF) format. All collected structures were imported to the Maestro Molecular Modeling Suite of Schrödinger (version 11.2) and prepared and energy-minimized using the OPLS2005 force field [13] with the LigPrep module (Schrödinger Release 2018-2: LigPrep, Schrödinger, LLC, New York, NY, USA, 2018). Then, the phytochemical structures were imported into the Qikprop module (Schrödinger Release 2018-2: Qikprop, Schrödinger, LLC, New York, NY, USA, 2018) to screen molecules based on their ADMET drug-likeness properties. The Qikprop module assesses each compound with the ADMET-relevant descriptors and provides a compliance score. The compounds that had a QikProp stars score of less than 3 were selected to have good drug-likeness properties. The QikProp stars score indicates the number of property/descriptor values that deviate from the 95% range of similar values observed in known drugs. A high stars score indicates that the molecule is less similar to known drugs compared with molecules with fewer stars score. In total, fifty descriptors are taken into account when determining the stars score including molecular weight, donor hydrogen bonds, acceptor hydrogen bonds, water partition coefficient, and aqueous solubility [14]. Then, the screened compounds were subjected to molecular docking.

2.4. Protein Preparation

The X-ray crystallographic protein structure (PDB ID: 1GRI) [15] was searched and downloaded in PDB format from the Protein Data Bank (PDB) (https://www.rcsb.org/, accessed on 5 August 2023) [16]. The retrieved structure was observed to be dimeric, consisting of chains A and B with 217 amino acids per chain. Each chain contains two SRC homology 3 domains (SH3, residues (1–58) and (156–215), and one SH2 domain localized between 60–152 residues). From the downloaded GRB2 (PDB ID: 1GRI) protein, two distinct

structures (1: dimeric (Chain A and B) and 2: monomeric (Chain B)) were constructed for further analysis. Both the structures (dimeric and monomeric) were prepared, and the missing residues (28–33), hydrogen atoms, and side chains were added using the Protein Preparation Wizard of Maestro (Schrödinger Release 2018-2, Schrödinger, LLC, New York, NY, USA, 2018). The PROPKA tool (Schrödinger Release 2018-2, Schrödinger, LLC, New York, NY, USA, 2018), as implemented in Maestro, was employed to generate an accurate ionization state under pH 7.4 conditions, and finally, the prepared structures were energy-minimized using the OPLS_2005 force field.

2.5. Molecular Docking

The docking site was defined by using the "Receptor Grid Generation" panel in Maestro 11.2 version, Schrödinger. The molecular docking was performed by constructing the grid of the monomeric and dimeric structures, respectively. Then, three independent docking experiments were performed: two for the monomeric and one for the dimeric GRB2 protein. For the monomeric structure, two independent grids were generated for docking: the grid (30 × 30 × 30 Å) around the SH2 domain at the peptide inhibitor site reported by Nioche et al., 2002 [17], and the grid box covering the complete monomeric structure that allows blind docking of phytochemicals at any possible sites of protein. Then, the blind docking for the dimeric structure was carried out by creating a grid box that encloses the complete dimeric protein structure. The phytochemicals with drug-like properties were docked using the Standard Precision (SP) setting in the Glide module (Schrödinger Release 2018-2: Glide, Schrödinger, LLC, New York, NY, USA, 2018) [18]. The phytochemical presenting the best predicted binding affinity (based on the Glide score) against the putative GRB2 target (monomer or dimeric) was chosen and investigated for its stability through MD simulation.

2.6. Molecular Dynamics Simulation

The stability of the dimer GRB2-piperbetol complex was investigated by performing MD simulation using the Desmond molecular dynamics (MD) engine, as implemented in Maestro (Schrödinger Release 2018-2: Desmond, Schrödinger, LLC, New York, NY, USA, 2018) [19]. The MD simulation of the docked complex employed the OPLS 2005 force-field [13]. The complex was positioned in an orthorhombic box at a 10 Å distance from the box edges, and the box was filled with TIP3P water molecules [20]. The box volume for the periodic boundary conditions was determined based on the complex type, and counter ions (Na^+ or Cl^-) were randomly added to neutralize the system. Furthermore, the default 0.15 M NaCl was added to maintain the physiological environment. The solvated system was minimized, followed by the default relaxation protocol of Desmond, as implemented in Maestro. Next, the system was simulated 100 ns using the Berendsen NVT ensemble [21], maintaining a temperature of 10 K, and keeping the heavy atoms on the solute restrained. Subsequently, the production MD simulation of 100 ns was performed in triplicate at a temperature of 300 K, with a pressure of 1 atm. Thermostat relaxation time was 1 ps and the barostat relaxation time was 2 ps, both coupled under isothermal isobaric ensemble (NPT). The Nosé–Hoover thermostat [22] and the Martyna-Tobias-Klein barostat [23] were employed to control the temperature and pressure. The simulation trajectory coordinates were saved at intervals of 100 ps. Then, the MD trajectories were analyzed with respect to root-mean-square deviation (RMSD), root-mean-square fluctuation (RMSF), and protein–ligand contacts were assessed to determine the stability of the complex.

3. Results

3.1. Target Selection and Enrichment Analysis

In total, 9455 CAD-associated genes were gathered from the above-mentioned databases, and the protein network was constructed using Cytoscape 3.9.1. The constructed network resulted in 9455 nodes and 17,486 edges. Further, the network was dissected into multiple hubs, of which the GRB2 protein was noticed to have a higher degree of connectivity

with 246 proteins. Further, the hub enrichment analysis was executed for GRB2 and its interconnected proteins with an FDR value < 0 05. Figure 2 represents the top 20 biological processes, cellular components, molecular functions, and molecular pathways of the GRB2 hub proteins that were significantly linked with CAD pathogenesis. Based on this, the GRB2 protein could be the putative drug target that influences most of the proteins associated with the CAD pathogenesis. Following that, the GRB2 protein structure was retrieved from the PDB database (PDB ID: 1GRI) (Figure 3) and established as having monomeric and dimeric structures, as detailed in the Section 2 for molecular docking.

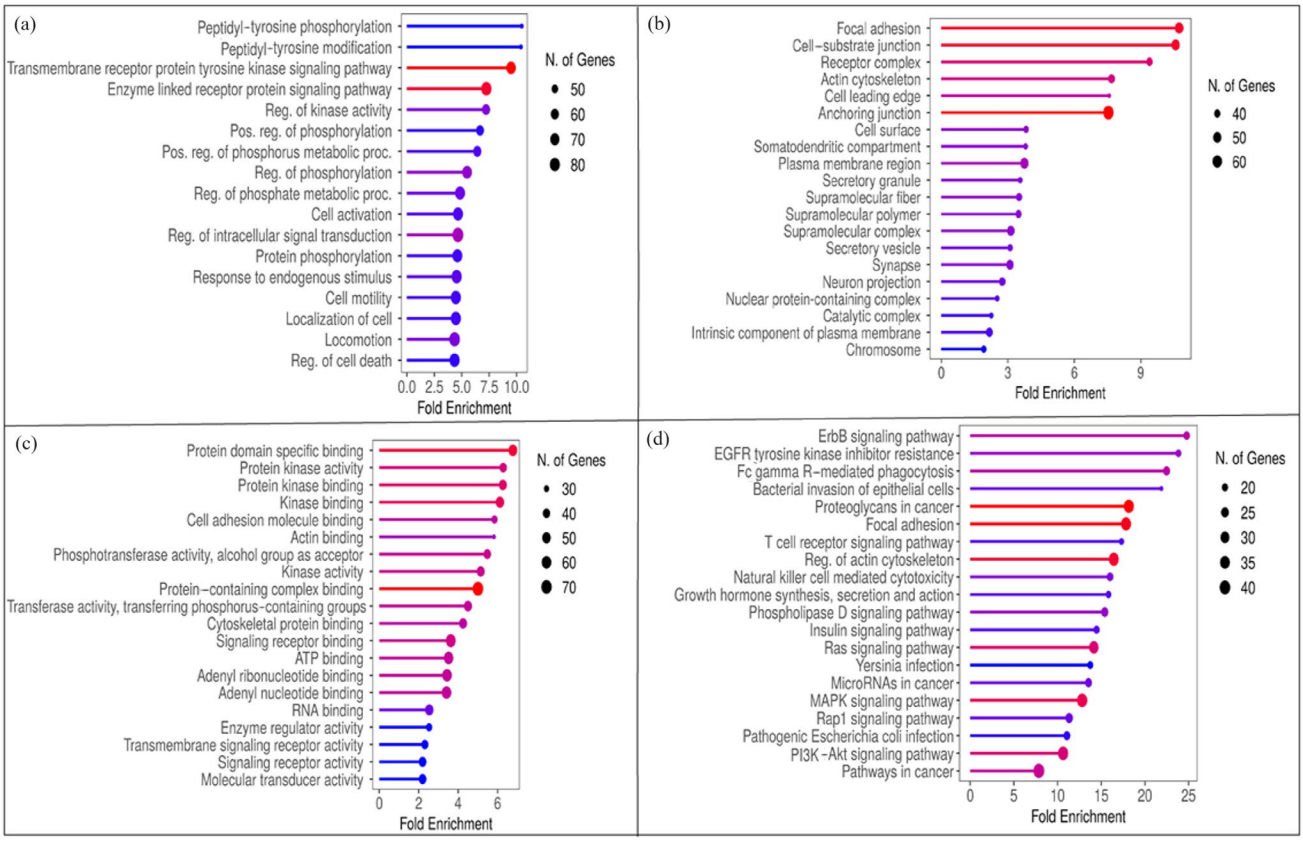

Figure 2. Gene enrichment analysis: (**a**) Biological processes, (**b**) cellular components, (**c**) molecular functions, and (**d**) KEGG pathways.

3.2. ADMET and Docking Analysis

A total of 111 phytochemicals of *Piper betle* (L.) were listed in the IMPPAT database, and their structures were retrieved from the IMPPAT in SDF format. Then, these 111 phytochemicals were subjected to Qikprop to screen them based on their ADMET properties. Consequently, the 49 phytochemicals with the lowest QikProp stars score ($\leq$3) were selected (Table S1). The phytochemicals with the lowest stars score are most likely to have similar pharmacological properties to the existing drugs [14]. Three independent docking experiments (two docking experiments at the monomeric and one at the dimeric GRB2 structure) were performed. The Glide docking scores of the docked compounds were compared to select the compounds predicted to bind the best to the GRB2 protein. Among the 49 phytochemicals, piperbetol showed the best Glide score (−8.10 kcal/mol) with the dimeric GRB2 (Figure 4) (Table 1), whereas no better Glide score was observed for any compound docked at the monomeric structures. As a result, the piperbetol-dimeric GRB2 complex was chosen for the MD simulation.

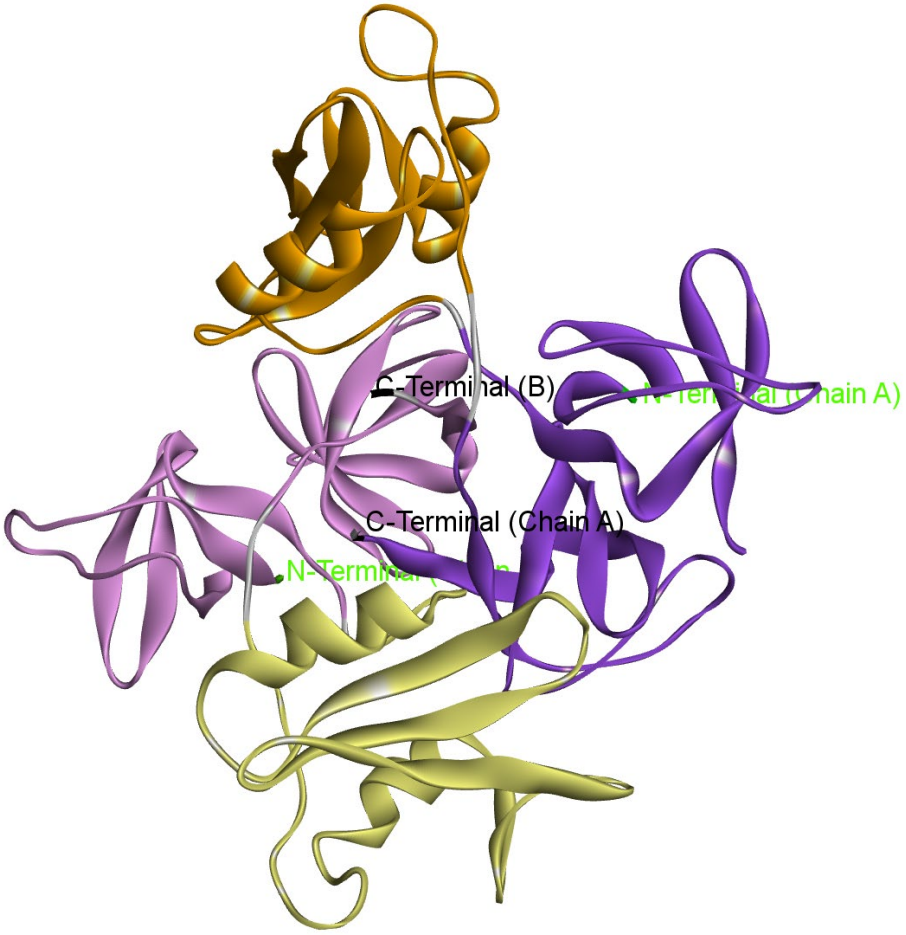

Figure 3. Dimeric structure of GRB2 with N and C terminals (PDB ID: 1GRI); Chain A: SH2 domain (orange) and SH3 domain (violet); Chain B: SH2 domain (yellow) and SH3 domain (pink).

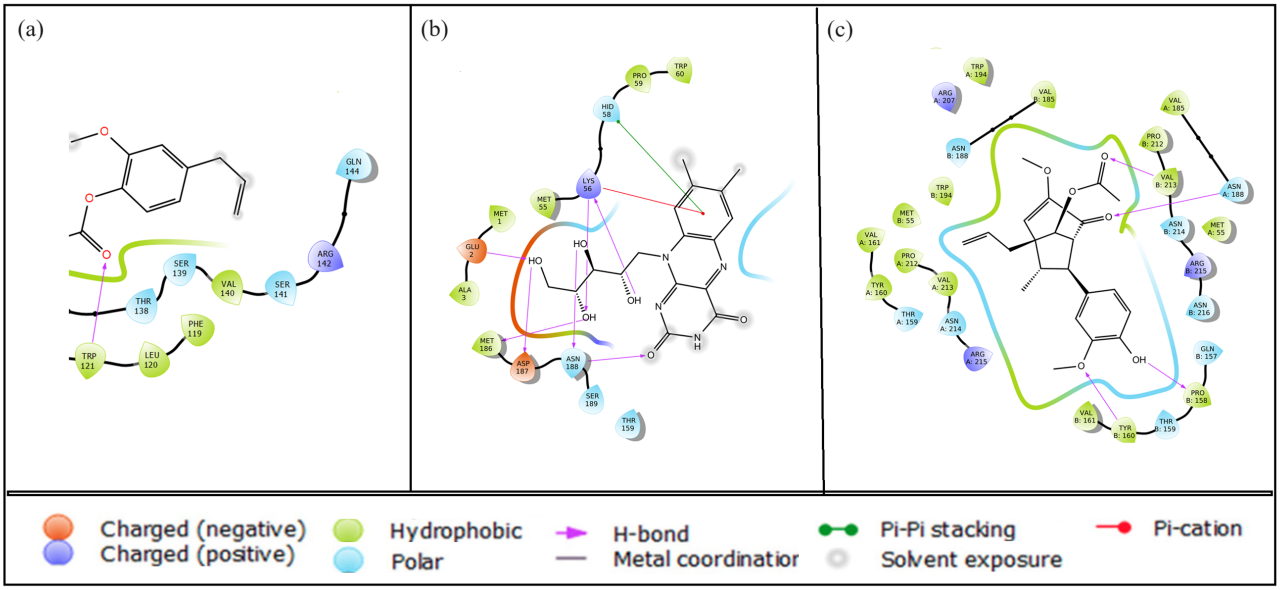

Figure 4. (**a**) Two-dimensional interaction diagram of acetyleugenol with the monomeric GRB2 structure, docked at the peptide inhibitor binding site at the SH2 domain; (**b**) interactions of riboflavin with the monomeric GRB2 structure, docked blindly at the monomeric GRB2; and (**c**) interactions of piperbetol with the dimeric GRB2 structure, docked blindly at the dimeric GRB2 structure.

Table 1. The top three docking results of *Piper betle* (L.) compounds.

SH2 Domain Binding		
Compound ID	**Compound Name**	**Glide Score (Kcal/mol)**
IMPHY006709	Acetyleugenol	−5.12
IMPHY001144	Dillapiol	−4.95
IMPHY000846	Riboflavin	−4.58
Binding score with monomeric GRB2		
IMPHY000846	Riboflavin	−6.37
IMPHY017327	p-Menthane-1,3-diol	−5.78
IMPHY001246	Carvacrol	−5.28
Binding score with dimeric GRB2		
IMPHY001073	Piperbetol	−8.10
IMPHY002191	Piperol B	−7.68
IMPHY008892	Methyl piperbetol	−7.37

3.3. MD Simulation

Through MD simulation, the stability of the piperbetol-GRB2 dimeric complex was evaluated for 100 ns. The protein's RMSD during the MD simulation is shown in Figure 5. The corresponding ligand RMSD for piperbetol is plotted in the same figure. The average RMSD (C-alpha) of GRB2 over 100 ns was 3.31 nm (Figure 5), suggesting that piperbetol and GRB2 formed a stable complex during the simulation. In a similar manner, the RMSF plot depicts the protein residues' fluctuation upon ligand binding. In our case, the RMSF plot (Figure 6) of the GRB2 protein demonstrates increased fluctuation at the ASP14 and GLN34 residues in chain A and ASP14, GLN34, and ASP172 residues in chain B. These residues are located in the SH3 domains' flexible loop regions. Particularly, the residues ASN188 (chain A), PRO158 (chain B), TYR160 (chain B), and VAL213 (chain B) displayed RMSF values of 1.52, 0.87, 0.68, and 1.12 nm at the binding site of piperbetol. These residues' generally low fluctuation strongly supports the binding of piperbetol with the GRB2 at this binding pocket, which is found at the dimer interface of GRB2 (Figures 4c and 6). In addition, our protein–ligand contact analysis revealed three types (hydrogen bond, hydrophobic, and water bridges) of interactions between piperbetol and GRB2. Notably, chain A demonstrated 12 interactions, whereas chain B created 16 contacts with piperbetol (Figures 4c and 7). In chain A, hydrogen bond formation was shown to be predominant, whereas water-mediated interactions in chain B were frequent and had a significant impact on piperbetol binding (Figure 7). Additionally, it appears that piperbetol interactions, especially with ARG215 (chain A), TRP194 (chain A), ASN188 (chain A), and VAL213 (chain B), are well maintained throughout the simulation period (100 ns) (Figures 8 and 9). Further, two parallel simulations were conducted for better sampling, which showed a similar behavior to the primary simulation (Figures S1–S10).

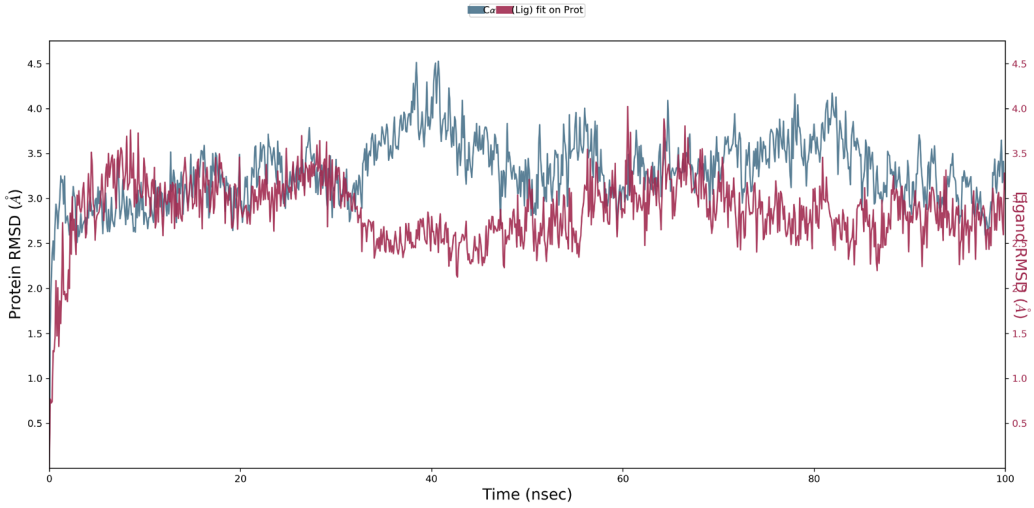

Figure 5. The plot depicts the root-mean-square deviation (RMSD) of the C-alpha atoms of the GRB2 protein and the RMSD of the ligand piperbetol in the piberbetol-GRB2 complex over a 100 ns simulation.

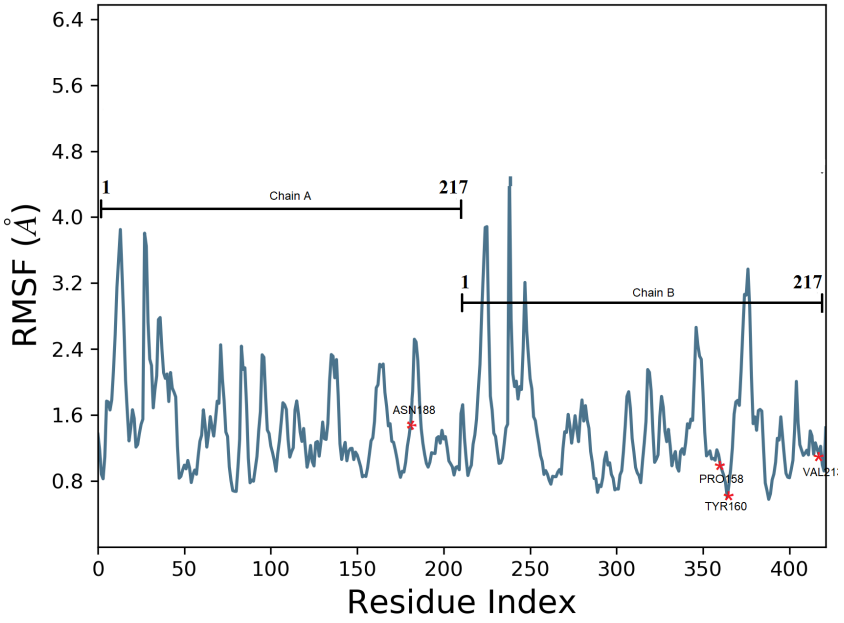

Figure 6. A plot depicting the persistence of residual flexibility as root-mean-square fluctuation (RMSF) over a 100 ns interval. Chain A and Chain B of GRB2 dimer each contain 217 amino acids, with the * representing the piperbetol binding site.

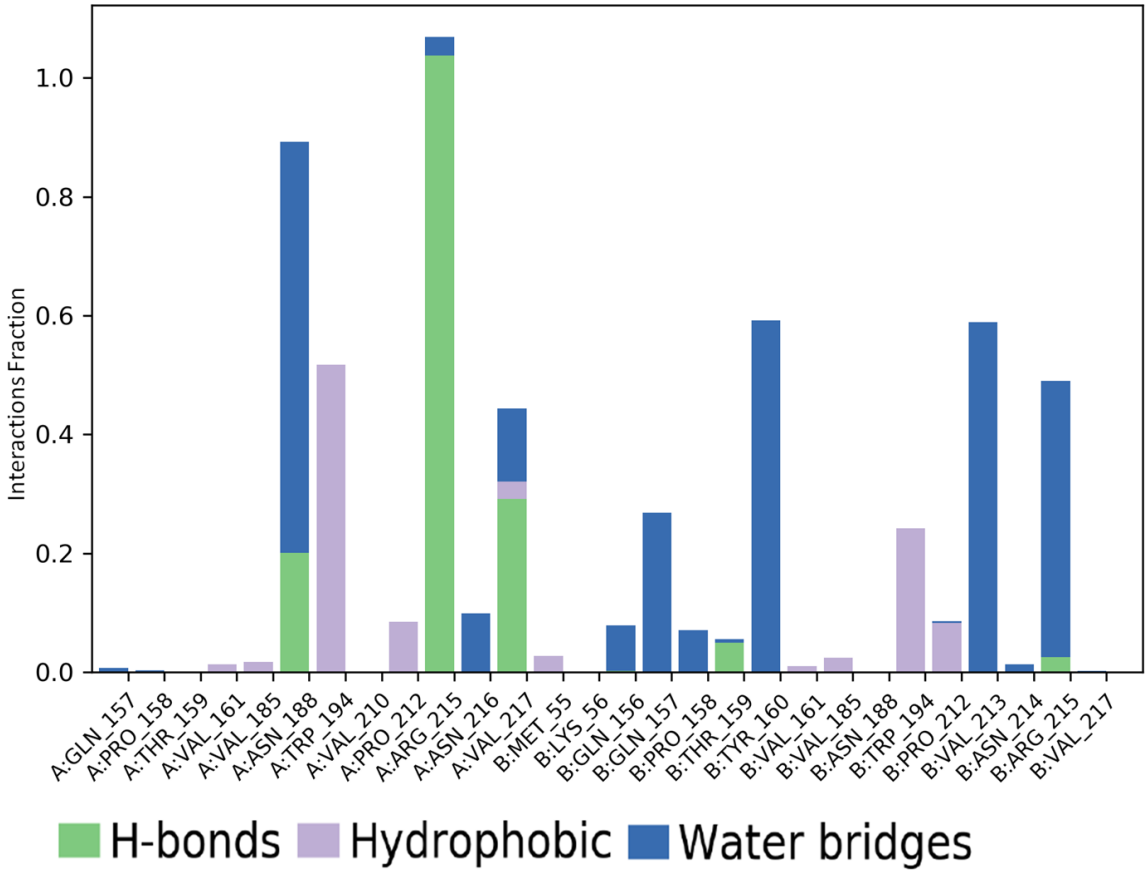

Figure 7. Protein–ligand contact analysis revealed three types (hydrogen bond, hydrophobic, and water bridges) of interactions between piperbetol and GRB2 protein.

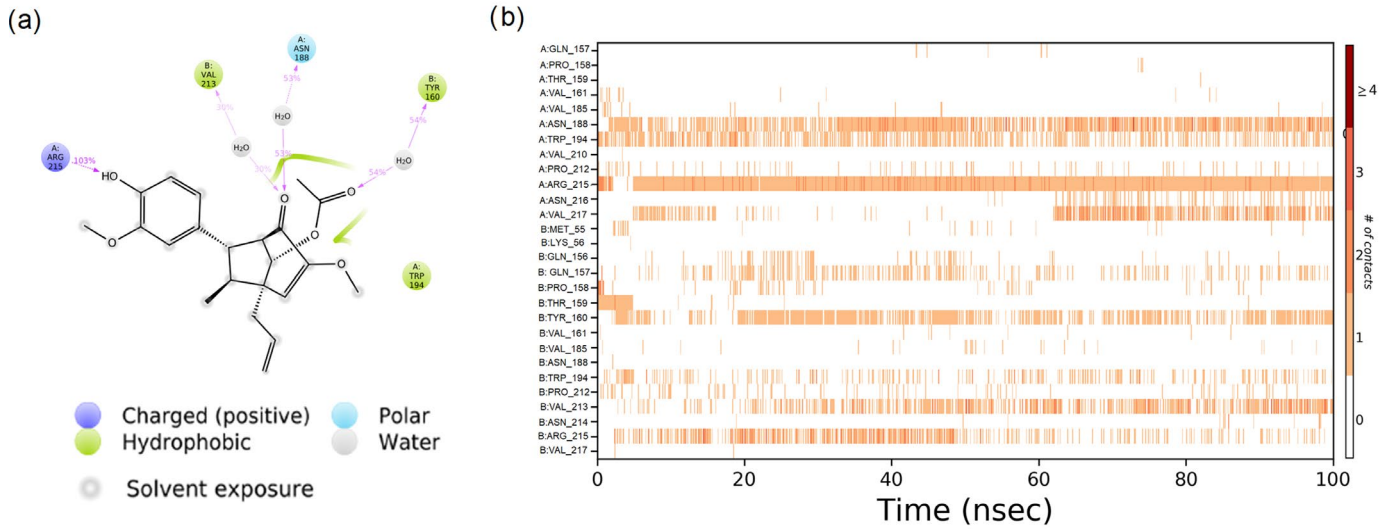

Figure 8. Protein–ligand contacts during a 100 ns MD simulation. (**a**) Persistent ligand interactions with the protein residues. (**b**) Persistency of ligand–protein contacts in the piperbetol-GRB2 complex during 100 ns.

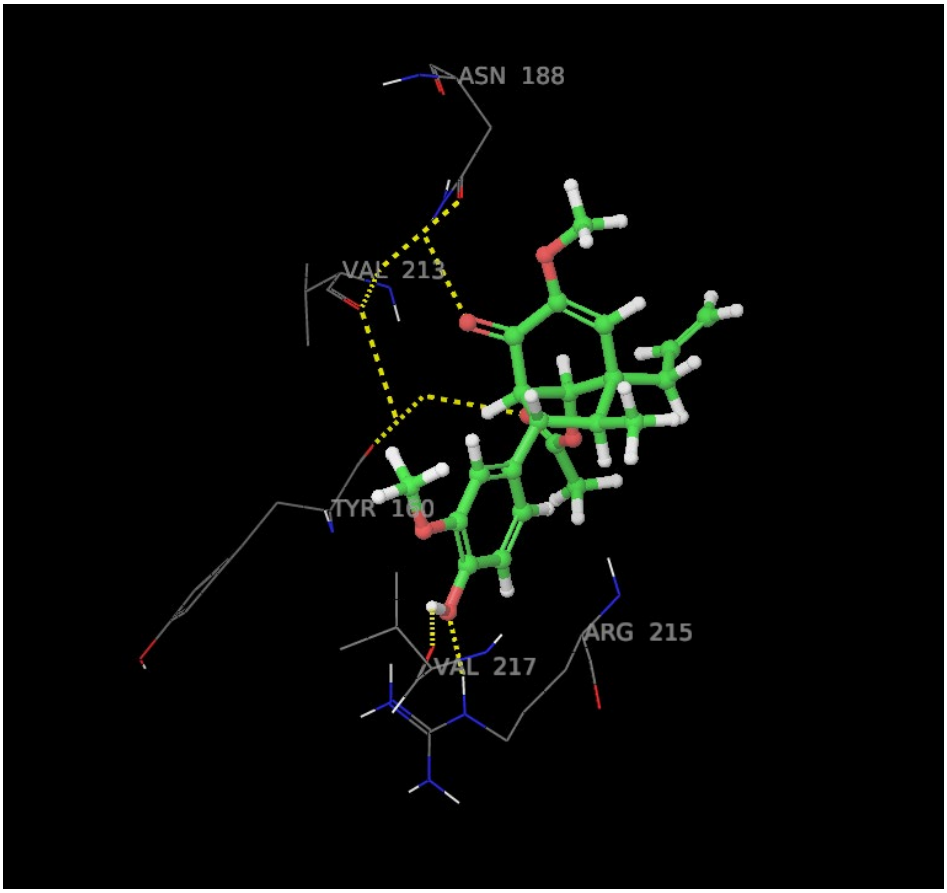

Figure 9. Three-dimensional view of the piperbetol-GRB2 dimer complex interactions captured in the final frame of the MD simulation trajectory. Yellow dashed lines represent hydrogen bond contacts.

4. Discussion

CAD is one of the most common diseases, with a reported high mortality rate worldwide. Currently, several drugs are being used to treat CAD [24]. Despite the effectiveness of these medications, the high mortality rate implies the presence of undiscovered pharmacological targets that require exploration to improve treatment efficacy. As a result, the current study is focused on identifying the pharmacological target through protein network analysis and discovering possible potent inhibitors sourced from traditional medicinal plants. Recently, researchers have been focusing on natural-plant-derived compounds to treat various diseases. Serafini et al. (2016) reported that the food-based medicinal plants *Zingiber officinale*, *Silybum marianum*, *Crataegus monogyna*, *Passiflora edulis*, and *Matricaria chamomilla* have anti-oxidant and anti-inflammatory activities [25]. Similarly, Seo et al., 2022, report that *Piper betle* (L.) compounds can inhibit inflammatory targets that could benefit inflammatory diseases, including NF-κB, MAPK, IL-1β, IL-6, and Nrf2 [26].

Herein, a well-known, ancient medicinal anti-inflammatory plant, *Piper betle* (L.), was selected to establish the beneficial role of its phytochemicals in CAD. *Piper betle* (L.) is a natural plant belonging to the kingdom plantae, piperaceae family. *Piper betle* is commonly known as betel vine, *Piper betle*, and *Piper betle* [27]. Several studies suggest that the benefits of *Piper betle* (L.) play a major role in the inhibition of platelet aggregation and wound repair, and that they have hepato-protective, antimicrobial, gastro-protective, antioxidant, anti-fertility, anti-diabetic, and anti-motility properties [28]. Dasagupta and De, 2004, reported the presence of phytochemicals in the leaves such as phenols, betelphenol, hydroxychavicol, cadinene, chavibetol, and chavicol, which have antioxidant, anti-inflammatory, and anti-carcinogenic properties [29]. Similar to this, Arya et al., 2010, demonstrated that *Piper betle* (L.) extract had cardioprotective effects on the recovery of

hemodynamics and ventricular functions following myocardial infarction [11]. However, these investigations do not address any specific phytochemicals against CAD targets in the improvement of the cardiovascular system. Therefore, this study utilizes the benefit of a computational approach to screen phytochemicals from *Piper betle* (L.) against a CAD target.

In total, we have retrieved 9455 genes by using keywords related to "coronary artery disease" from the Gene cards, OMIM, NCBI, DisGeNET, intAct, MINT, BioGRID, and String databases. From the collected genes, the protein interaction network was constructed. Following from this, GRB2 has been selected as a potential therapeutic target by using protein network analysis. Further, GRB2-interconnected proteins were utilized for functional enrichment analysis. Notably, most biological processes involving the GRB2-connected proteins were linked with CAD pathogenesis, such as intracellular signal transduction, locomotion, enzyme-linked receptor protein signaling pathways, the response to endogenous stimuli, and cell death. Likewise, the molecular function consists of a protein-containing complex binding, signaling receptor-binding proteins, adenyl ribonucleotide binding, adenyl nucleotide binding, and ATP binding. Similarly, the cellular components include anchoring junctions, focal adhesion, cell substrate junctions, plasma membrane regions, and supramolecular complexes. Additionally, the assessment based on the molecular pathways of the GRB2 hub proteins suggest that they play a role in mitogen-activated protein kinase (MAPK), the Ras signaling pathway, the phosphatidylinositol-3 kinase-Serine/threonine-protein kinase (PI3K-AKT) signaling pathway, and focal adhesion. Overall, our results are in accordance with Mitra et al., 2018, which highlights the role of GRB2 in the activation of downstream MAPK pathways [30]. Moreover, Maignan et al. reported on the adapter protein GRB2, which binds to the mammalian growth factor receptor and plays a crucial role in initiating guanine nucleotide exchange on the Ras signaling pathway [15]. GRB2 interacts with the Ras receptor via its SH2 domain and with the carboxyl-terminal domain of Son of sevenless through its two SH3 domains, making it a pivotal component in the signal transduction pathway [15]. Interestingly, our molecular pathway analysis also found that the Ras signaling pathway is involved in CAD progression. Proctor et al. (2007) demonstrated the necessity of GRB2 for atherosclerotic lesion formation through oxidized LDL uptake by macrophages in a mice model [31]. Similarly, Dong et al. (2022) found increased serum GRB2 concentrations in individuals with both T2DM and carotid atherosclerosis (CAS) [32]. Also, they observed a linear correlation between the serum GRB2 level and carotid intima-media thickness, indicating the potential involvement of GRB2 in the development of T2DM with CAS [32]. Additionally, Wang et al. (2021) established the link between cardiorenal syndrome type 3 (CRS-3) and elevated IL-6/GRB2, which plays an important role in cardiac dysfunction by suppressing the Akt/mTOR signaling pathway and inducing impairment in cardiomyocyte mitochondrial bioenergetics [33]. Therefore, targeting GRB2 might be beneficial in treating CAD.

We searched for effective small molecules to inhibit the GRB2 protein. To do so, we screened hundreds of *Piper betle* (L.) compounds by employing the ADMET compliance score (stars score): drug likeness parameters (stars score range: 0 to 3), molecular weight (range: 130.0 to 725.0), hydrogen bond donor (range: 0.0 to 6.0), hydrogen bond acceptor (range: 2.0 to 20.0), log P (range: −2.0 to 6.5), predicted aqueous solubility (range: −6.5 to 0.5), Caco cell permeability (range: <25 is poor and >500 is great), central nervous system activity (−2 (inactive) to +2 (active)), brain/blood partition coefficient (range: −3.0 to 1.2), apparent MDCK cell permeability (range: <25 is poor and >500 is great), percentage of human oral absorption (range: <25 is poor and >80% is high), human serum albumin binding (range: –1.5 to 1.5), number of likely metabolic reactions (range: 1 to 8), IC50 value for blockage of HERG K+ channels (concern < –5), number of violations of Lipinski's rule of five (maximum is four), and number of violations of Jorgensen's rule of three (maximum is three) [34]. Based on these parameters, 49 phytochemicals were filtered from the 111 *Piper betle* (L.) compounds and assessed through molecular docking. The docking results showed that the interaction of acetyleugenol with the SH2 domain of GRB2 has a Glide score of −5.12 kcal/mol. Likewise, riboflavin scored −6.37 kcal/mol with monomeric

GRB2, while the piperbetol had the best predicted binding affinity (−8.10 kcal/mol) at the dimeric GRB2. Piperbetol formed hydrogen bonds with the GRB2 residues (Chain B: PRO158, TYR160, VAL213 and Chain A: ASN188). Interestingly in our study, the binding site of piperbetol was formed by both chain A and Chain B. Likewise, the MD simulation showed a stable conformation (RMSD) of the piperbetol-GRB2 complex and less protein flexibility (RMSF) [35], which allows piperbetol to form a constant interaction with SH3 domains at Chain A (ASN188, TRP194, ARG215, and VAL217) and Chain B (TYR160, VAL213, and ARG215). Interestingly, our molecular docking and MD simulation results suggest a constant interaction of piperbetol with TYR160, which might have an effect on the dimer dissociation. Ahmed et al. demonstrate the influence of TYR160 phosphorylation contributing to the dimer dissociation of GRB2 [36]. Thus, piperbetol binding with dimeric GRB2 might affect the protein dimer formation, which may alter its function. Zeng et al. (1997) demonstrated the effect of piperbetol in inhibiting the platelet aggregation in a rabbit model [37]. Similarly, Haslan et al. (2015) reported that piperbetol has an anti-oxidant property that reduces pro-thrombotic activity, which contributes to cardioprotective action [38]. Considering these reports and the results of our investigation, it is plausible that piperbetol may have pharmacological effects related primarily to the treatment of CAD, as piperbetol was the best scored compound among the docked *Piper betle* (L.) compounds with dimeric GRB2. We further investigated the stability of the predicted binding complex using MD simulation, which showed a stable conformation between piperbetol and dimeric GRB2 over a 100 ns period. Additionally, parallel simulations were conducted using different random seeds, which showed similar behavior to the primary simulation (Figures S1–S10). Particularly, parallel simulations 1 and 2 have average RMSD values of 3.06 nm and 3.36 nm, while the primary simulation has an average of 3.31 nm. Also, the RMSF values of both the primary and parallel simulations showed a similar pattern of amino acid fluctuations at the piperbetol binding sites (Figure S10). Overall, based on the MD simulation, we can conclude that the *Piper betle* (L.) compound piperbetol formed a stable complex with the dimeric GRB2 during the 100 ns simulation.

5. Conclusions

In conclusion, our protein network analysis suggests that GRB2 could be a potential therapeutic target for anti-CAD therapies. Our molecular docking and MD simulation studies suggest that piperbetol of *Piper betle* (L.) interacts with the dimeric GRB2, which might affect the dimer formation. Hence, piperbetol could serve as a phytochemical hit compound from *Piper betle* (L.) for the development of novel anti-CAD drugs. However, in vitro studies are essential to validate our findings and investigate the therapeutic efficacy of piperbetol against CAD.

Supplementary Materials: The following supporting information can be downloaded at: https://www.mdpi.com/article/10.3390/pr11113064/s1. Figure S1: Root mean square deviation of piperbetol with dimeric GRB2 during 100 ns molecular dynamics simulation; Figure S2: Root mean square fluctuation of piperbetol with dimeric GRB2 during 100 ns molecular dynamics simulation; Figure S3: Protein-ligand contacts of piperbetol with dimeric GRB2 during 100 ns molecular dynamics simulation; Figure S4: Timeline representation of piperbetol with dimeric GRB2 contacts during 100 ns molecular dynamics simulation; Figure S5: Root mean square deviation of piperbetol with dimeric GRB2 during 100 ns molecular dynamics simulation; Figure S6: Root mean square fluctuation of piperbetol with dimeric GRB2 during 100 ns molecular dynamics simulation; Figure S7: Protein-ligand contacts of piperbetol with dimeric GRB2 during 100 ns molecular dynamics simulation; Figure S8: Timeline representation of piperbetol with dimeric GRB2 contacts during 100 ns molecular dynamics simulation; Figure S9: Bar graph showing the RMSD (C-α) average and standard deviation for the dimer GRB2 with piperbetol presenting no differences in the trajectories in both primary and parallel simulation during 100 ns; Figure S10: The Line graph present RMSF value of amino acids at piperbetol binding sites with dimeric GRB2. Both the primary and parallel simulations shows similar pattern of fluctuation confirming the consistency in simulation results. Table S1: Screened ADMET properties for 49 *Piper betle* compounds.

Author Contributions: S.S.S.J.A. designed and interpreted the study. S., J., S.F.A. and A.W. carried out the investigation, formal analysis, and data curation. All authors have read and agreed to the published version of the manuscript.

Funding: This research was funded by Researchers Supporting Project Number (RSPD2023R709).

Data Availability Statement: Not applicable.

Acknowledgments: All authors thank their institutes for the infrastructure support for this study. The authors acknowledge and extend their appreciation to the Researchers Supporting Project Number (RSPD2023R709), King Saud University, Riyadh, Saudi Arabia for funding this study.

Conflicts of Interest: The authors declare no conflict of interest.

References

1. Monisha, K.G.; Prabu, P.; Chokkalingam, M.; Murugesan, R.; Milenkovic, D.; Ahmed, S.S.S.J. Clinical utility of brain-derived neurotrophic factor as a biomarker with left ventricular echocardiographic indices for potential diagnosis of coronary artery disease. *Sci. Rep.* **2020**, *10*, 16359. [CrossRef]
2. Ralapanawa, U.; Sivakanesan, R. Epidemiology and the magnitude of coronary artery disease and acute coronary syndrome: A narrative review. *J. Epidemiol. Glob. Health* **2021**, *11*, 169. [CrossRef]
3. Hajar, R. Risk factors for coronary artery disease: Historical perspectives. *Heart Views* **2017**, *18*, 109. [CrossRef]
4. Findley, A.S.; Richards, A.L.; Petrini, C.; Alazizi, A.; Doman, E.; Shanku, A.G.; Davis, G.O.; Hauff, N.; Sorokin, Y.; Wen, X.; et al. Interpreting coronary artery disease risk through gene–environment interactions in gene regulation. *Genetics* **2019**, *213*, 651–663. [CrossRef]
5. Tantry, U.S.; Navarese, E.P.; Bliden, K.P.; Gurbel, P.A. Acetylsalicylic acid and clopidogrel hyporesponsiveness following acute coronary syndromes. *Kardiol. Pol.* **2018**, *76*, 1312–1319. [CrossRef]
6. Shaito, A.; Thuan, D.T.; Phu, H.T.; Nguyen, T.H.; Hasan, H.; Halabi, S.; Abdelhady, S.; Nasrallah, G.K.; Eid, A.H.; Pintus, G. Herbal medicine for cardiovascular diseases: Efficacy, mechanisms, and safety. *Front. Pharmacol.* **2020**, *7*, 422. [CrossRef] [PubMed]
7. Sofowora, A.; Ogunbodede, E.; Onayade, A. The role and place of medicinal plants in the strategies for disease prevention. *Afr. J. Tradit. Complement. Altern. Med.* **2013**, *10*, 210–229. [CrossRef]
8. Nayaka, N.M.; Sasadara, M.M.; Sanjaya, D.A.; Yuda, P.E.; Dewi, N.L.; Cahyaningsih, E.; Hartati, R. *Piper betle* (L): Recent review of antibacterial and antifungal properties, safety profiles, and commercial applications. *Molecules* **2021**, *26*, 2321. [CrossRef] [PubMed]
9. Murugesan, S.; Ravichandran, D.; Lakshmanan, D.K.; Ravichandran, G.; Arumugam, V.; Raju, K.; Geetha, K.; Thilagar, S. Evaluation of anti-rheumatic activity of *Piper betle* L. (Betelvine) extract using in silico, in vitro and in vivo approaches. *Bio. Org. Chem.* **2020**, *103*, 104227. [CrossRef]
10. Ng, P.L.; Rajab, N.F.; Then, S.M.; Yusof, Y.A.; Ngah, W.Z.; Pin, K.Y.; Looi, M.L. Piper betle leaf extract enhances the cytotoxicity effect of 5-fluorouracil in inhibiting the growth of HT29 and HCT116 colon cancer cells. *J. Zhejiang Univ. Sci. B* **2014**, *15*, 692. [CrossRef]
11. Arya, D.S.; Arora, S.; Malik, S.; Nepal, S.; Kumari, S.; Ojha, S. Effect of *Piper betle* on cardiac function, marker enzymes, and oxidative stress in isoproterenol-induced cardiotoxicity in rats. *Toxicol. Mech. Methods* **2010**, *20*, 564–571. [CrossRef] [PubMed]
12. Mohanraj, K.; Karthikeyan, B.S.; Vivek-Ananth, R.P.; Chand, R.P.B.; Aparna, S.R.; Mangalapandi, P.; Samal, A. IMPPAT: A curated database of Indian Medicinal Plants, Phytochemistry and Therapeutics. *Sci. Rep.* **2018**, *8*, 4329. [CrossRef] [PubMed]
13. Banks, J.L.; Beard, H.S.; Cao, Y.; Cho, A.E.; Damm, W.; Farid, R.; Felts, A.K.; Halgren, T.A.; Mainz, D.T.; Maple, J.R.; et al. Integrated Modeling Program, Applied Chemical Theory (IMPACT). *J. Comp. Chem.* **2005**, *26*, 1752. [CrossRef]
14. Schrödinger. *QikProp User Manual*; Schrödinger Press: Cambridge, MA, USA, 2015. Available online: http://gohom.win/ManualHom/Schrodinger/Schrodinger_2015-2_docs/qikprop/qikprop_user_manual.pdf (accessed on 2 August 2023).
15. Maignan, S.; Guilloteau, J.P.; Fromage, N.; Arnoux, B.; Becquart, J.; Ducruix, A. Crystal structure of the mammalian Grb2 adaptor. *Science* **1995**, *268*, 291–293. [CrossRef] [PubMed]
16. Berman, H.M.; Westbrook, J.; Feng, Z.; Gilliland, G.; Bhat, T.N.; Weissig, H.; Shindyalov, I.N.; Bourne, P.E. The Protein Data Bank. *Nucleic Acids Res.* **2000**, *28*, 235–242. [CrossRef] [PubMed]
17. Nioche, P.; Liu, W.Q.; Broutin, I.; Charbonnier, F.; Latreille, M.T.; Vidal, M.; Roques, B.; Garbay, C.; Ducruix, A. Crystal structures of the SH2 domain of Grb2: Highlight on the binding of a new high-affinity inhibitor. *J. Mol. Biol.* **2002**, *315*, 1167–1177. [CrossRef]
18. Friesner, R.A.; Murphy, R.B.; Repasky, M.P.; Frye, L.L.; Greenwood, J.R.; Halgren, T.A.; Sanschagrin, P.C.; Mainz, D.T. Extra Precision Glide: Docking and Scoring Incorporating a Model of Hydrophobic Enclosure for Protein-Ligand Complexes. *J. Med. Chem.* **2006**, *49*, 6177–6196. [CrossRef]
19. Bowers, K.J.; Chow, E.; Xu, H.; Dror, R.O.; Eastwood, M.P.; Gregersen, B.A.; Shaw, D.E. Scalable algorithms for molecular dynamics simulations on commodity clusters. In Proceedings of the 2006 ACM/IEEE Conference on Supercomputing, Tampa, FL, USA, 11–17 November 2006; p. 84-es.
20. Jorgensen, W.L.; Chandrasekhar, J.; Madura, J.D.; Impey, R.W.; Klein, M.L. Comparison of simple potential functions for simulating liquid water. *J. Chem. Phys.* **1983**, *79*, 926–935. [CrossRef]

21. Berendsen, H.J.C.; Postma, J.P.M.; van Gunsteren, W.F.; DiNola, A.; Haak, J.R. Molecular dynamics with coupling to an external bath. *J. Chem. Phys.* **1984**, *81*, 3684–3690. [CrossRef]
22. Evans, D.J.; Holian, B.L. The Nose-Hoover Thermostat. *J. Chem. Phys.* **1985**, *83*, 4069–4074. [CrossRef]
23. Martyna, G.J.; Tobias, D.J.; Klein, M.L. Constant pressure molecular dynamics algorithms. *J. Chem. Phys.* **1994**, *101*, 4177–4189. [CrossRef]
24. Pello Lazaro, A.M.; Blanco-Colio, L.M.; Franco Pelaez, J.A.; Tunon, J. Anti-Inflammatory drugs in patients with ischemic heart disease. *J. Clin. Med.* **2021**, *10*, 2835. [CrossRef]
25. Serafini, M.; Peluso, I. Functional foods for health: The interrelated antioxidant and anti-inflammatory role of fruits, vegetables, herbs, spices and cocoa in humans. *Curr. Pharm. Des.* **2016**, *22*, 6701–6715. [CrossRef]
26. Seo, J.; Lee, U.; Seo, S.; Wibowo, A.E.; Pongtuluran, O.B.; Lee, K.; Han, S.B.; Cho, S. Anti-inflammatory and antioxidant activities of methanol extract of *Piper betle* Linn. (*Piper betle* L.) leaves and stems by inhibiting NF-κB/MAPK/Nrf2 signaling pathways in RAW 264.7 macrophages. *Biomed. Pharmacother.* **2022**, *155*, 113734. [CrossRef]
27. Biswas, P.; Anand, U.; Saha, S.C.; Kant, N.; Mishra, T.; Masih, H.; Bar, A.; Pandey, D.K.; Jha, N.K.; Majumder, M.; et al. Betelvine (*Piper betle* L.): A comprehensive insight into its ethnopharmacology, phytochemistry, and pharmacological, biomedical and therapeutic attributes. *J. Cell. Mol. Med.* **2022**, *26*, 3083–3119. [CrossRef]
28. Alam, B.; Akter, F.; Parvin, N.; Pia, R.S.; Akter, S.; Chowdhury, J.; Sifath-E-Jahan, K.; Haque, E. Antioxidant, analgesic and anti-inflammatory activities of the methanolic extract of Piper betle leaves. *Avicenna J. Phytomed.* **2013**, *3*, 112.
29. Dasgupta, N.; De, B. Antioxidant activity of *Piper betle* L. leaf extract in vitro. *Food Chem.* **2004**, *88*, 219–224. [CrossRef]
30. Mitra, P.; Kalailingam, P.; Tan, H.B.; Thanabalu, T. Overexpression of GRB2 enhances epithelial to mesenchymal transition of A549 cells by upregulating SNAIL expression. *Cells* **2018**, *7*, 97. [CrossRef] [PubMed]
31. Proctor, B.M.; Ren, J.; Chen, Z.; Schneider, J.G.; Coleman, T.; Lupu, T.S.; Semenkovich, C.F.; Muslin, A.J. Grb2 is required for atherosclerotic lesion formation. *Arterioscler. Thromb. Vasc. Biol.* **2007**, *27*, 1361–1367. [CrossRef]
32. Dong, Y.; Liu, J.; Ma, J.; Quan, J.; Bao, Y.; Cui, Y. The possible correlation between serum GRB2 levels and carotid atherosclerosis in patients with type 2 diabetes mellitus. *Front. Endocrinol.* **2022**, *13*, 963191. [CrossRef] [PubMed]
33. Wang, J.; Sun, X.; Wang, X.; Cui, S.; Liu, R.; Liu, J.; Fu, B.; Gong, M.; Wang, C.; Shi, Y.; et al. Grb2 Induces Cardiorenal Syndrome Type 3: Roles of IL-6, Cardiomyocyte Bioenergetics, and Akt/mTOR Pathway. *Front. Cell Dev. Biol.* **2021**, *9*, 630412. [CrossRef]
34. Jorgensen, W.L. Efficient Drug Lead Discovery and Optimization. *Acc. Chem. Res.* **2009**, *42*, 724–733. [CrossRef] [PubMed]
35. Daison, F.A.; Kumar, N.; Balakrishnan, S.; Venugopal, K.; Elango, S.; Sokkar, P. Molecular dynamics studies on the bacterial membrane pore formation by small molecule antimicrobial agents. *J. Chem. Inf. Model.* **2021**, *62*, 40–48. [CrossRef] [PubMed]
36. Ahmed, Z.; Timsah, Z.; Suen, K.M.; Cook, N.P.; Lee, G.R.; Lin, C.C.; Gagea, M.; Marti, A.A.; Ladbury, J.E. Grb2 monomer-dimer equilibrium determines normal versus oncogenic function. *Nat. Commun.* **2015**, *6*, 7354. [CrossRef]
37. Zeng, H.W.; Jiang, Y.Y.; Cai, D.G.; Bian, J.; Long, K.; Chen, Z.L. Piperbetol, methylpiperbetol, piperol A and piperol B: A new series of highly specific PAF receptor antagonists from *Piper betle*. *Planta Med.* **1997**, *63*, 296–298. [CrossRef] [PubMed]
38. Haslan, H.; Suhaimi, F.H.; Thent, Z.C.; Das, S. The underlying mechanism of action for various medicinal properties of *Piper betle* (betel). *Clin. Ter.* **2015**, *166*, 208–214.